THE JOURNAL OF PHYSICAL CHEMISTRY A

Article

pubs.acs.org/JPCA

Time-Resolved Studies of Charge Recombination in the Pyrene/TCNQ Charge-Transfer Crystal: Evidence for Tunneling

Robert J. Dillon and Christopher J. Bardeen*

Department of Chemistry, University of California, Riverside, Riverside, California 92521, United States

ABSTRACT: Previous studies of solid-state tetracyanobenzene-based donor–acceptor complexes showed that these materials were highly susceptible to both laser and mechanical damage that complicated the analysis of their electron-transfer kinetics. In this paper, we characterize the optical properties of a pyrene/tetracyanoquinodimethane charge-transfer crystal that is much more robust than the tetracyanobenzene compounds. This donor–acceptor complex has a charge-transfer absorption that extends into the near-infrared, rendering the crystal black. We use time-resolved fluorescence and diffuse reflectance transient absorption to study its dynamics after photoexcitation. We show that the initially excited charge-transfer state undergoes a rapid, monoexponential decay with a lifetime of 290 ps at room temperature. There is no evidence for any long-lived intermediate or dark states; therefore, this decay is attributed to charge recombination back to the ground state. Fluorescence lifetime measurements demonstrate that this process becomes temperature-independent below 60 K, indicative of a thermally activated tunneling mechanism. The subnanosecond charge recombination makes this low-band-gap donor–acceptor material a poor candidate for generating long-lived electron–hole pairs.

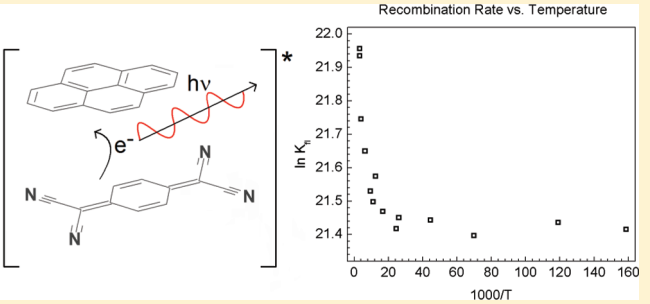

INTRODUCTION

Charge transfer (CT) in organic solid-state materials underlies many of the technological applications of these materials, from light-emitting diodes to photovoltaic cells. Molecular CT cocrystals, composed of alternating donor and acceptor molecules, provide a structurally well-defined medium in which the fundamental aspects of the CT process can be studied. Organic CT cocrystals and nanocrystals are also candidates for applications ranging from diodes to fluorescent probes.[1−3] In this work, we are concerned with crystals where the ground state consists of neutral donor and acceptor molecules and the CT only occurs in the excited state after absorption of a photon. These "nonionic" CT crystals (as classified by McConnell[4]) typically exhibit a relatively weak, red-shifted CT absorption band in addition to the absorption bands of their neutral constituents. The dynamics of CT complexes in solution have been extensively studied,[5−8] but there has been less work on their solid-state electron-transfer properties. We recently became interested in molecular CT crystals as highly ordered analogues for the bulk heterojunction polymer materials currently used in organic photovoltaics. Masuhara and others have shown that for many different CT complexes, the forward electron-transfer process occurs very rapidly, usually within a few hundred femtoseconds.[9−11] Early work by Kochi on crystalline powders composed of conjugated acene donor molecules and the electron acceptor tetracyanobenzene (TCNB) suggested that these initially formed CT states could dissociate into free carriers with high efficiencies.[12] Upon re-examination, however, it was found that the TCNB complexes were highly susceptible to both mechanical damage (resulting from grinding the crystals into powders) and photodamage (resulting from the high laser fluences used in transient absorption experiments).[13] We concluded that there was little evidence for rapid dissociation of the bound CT state formed after photoexcitation. For our further study of molecular CT crystals, we had two goals. First, we wanted to identify a more robust CT molecular crystal system, where mechanical and laser damage would have negligible effects on the kinetics. Second, we wanted to study the fate of the CT state created by photoexcitation in more detail and gain insight into the physical mechanism of charge recombination.

In order to achieve these two goals, we needed to identify a good model system. The previously identified problems with CT crystal stability were addressed by modifying the chemical system and preparation conditions. Rather than the fragile TCNB complexes, we turned to a different, higher molecular weight acceptor molecule, 7,7,8,8-tetracyanoquinodimethane (TCNQ). As our donor, we chose pyrene. The pyrene/TCNQ CT complex crystallizes in an alternating stacked geometry,[14] as shown in Figure 1, and its optical properties have been measured.[15] More interestingly, this crystal has been shown to have high photoconductivity relative to other CT crystals, suggesting that it can produce free carriers after photoexcitation.[16] The growth of single crystals of this material is straightforward, but making powdered samples whose properties mirrored those of the single crystal proved difficult.

Received: March 24, 2012
Revised: May 2, 2012

   dx.doi.org/10.1021/jp302829a | J. Phys. Chem. A XXXX, XXX, XXX–XXX

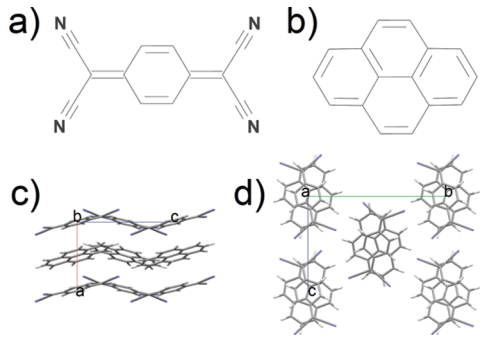

Figure 1. Chemical structures of (a) TCNQ and (b) pyrene and the crystal structure of pyrene/TCNQ (c) viewed from the side along the crystallographic *b* axis and (d) viewed from the top of the stacks along the crystallographic *a* axis.

Consistent data was obtained only for powders prepared using Teflon microbeads, rather than the usual $BaSO_4$ particles. We have characterized the absorption properties of the pyrene/TCNQ complex in both solution and in the crystalline state, showing that the CT absorbing state is similar in both. The solid-state luminescence decay is insensitive to both laser-induced photobleaching and to mechanical grinding, establishing this compound as being much more stable than its TCNB analogue. The similar luminescence properties of the powder and crystal forms allow us to correlate time-resolved luminescence and pump−probe measurements. We find that the 290 ps luminescence decay is exactly mirrored by the decay of the TCNQ radical anion absorption. Thus, the fluorescence decay reflects the rate of charge recombination back into the neutral ground state. By performing temperature-dependent fluorescence lifetime measurements, we find that this recombination is likely the result of an activated tunneling process involving a low-frequency vibrational mode, possibly a crystal phonon. This rapid nonradiative recombination channel helps explain why the yield of dissociated charges from the initially excited radical cation−anion pair is so small. Such rapid recombination provides a reason, in addition to the interdigitated crystal structure, for why the photoconductivity of these donor−acceptor systems tends to be quite low relative to polymer bulk heterojunction systems.

EXPERIMENTAL SECTION

Pyrene (Aldrich) and TCNQ (TCI America) were used as received. Pyrene/TCNQ crystals were readily grown by allowing an equimolar THF solution to slowly evaporate from a covered Petri dish left in the dark. Prior to covering, a few drops of xylenes were added to further retard the crystal growth process. Of the best crystals obtained, a few were set aside for single-crystal measurements, and several were mixed with Teflon powder (1 μm particle size, Aldrich) and pulverized in a mortar and pestle. The resultant powder was approximately 2% CT complex by mass.

The formation constant of the complex and the absorption coefficient for the CT band were calculated from the absorption spectra of solutions containing varying amounts of each. A 0.37 mM solution of TCNQ in chloroform was made and parceled out into eight vials, and the amount of solution added was carefully recorded. Into these eight solutions, varying amounts of pyrene were added to create a range of concentrations, from 12.1 to 648.1 mM. Pyrene was chosen as the varied constituent owing to its superior solubility in chloroform. A few milliliters of each sample was placed into a quartz cuvette, and the absorption was measured in a Cary 50 spectrometer.

Fluorescence lifetime experiments were performed on a 40 kHz Spectra Physics Spitfire laser system. Crystal samples were mounted on glass slides with a minimal amount of non-fluorescent vacuum grease. The fluorescence of powder samples was performed by sandwiching the powder between two glass slides. All experiments were performed under a vacuum of 10^{-4} Torr in a Janis ST-100 cryostat. The typical per-pulse fluence used was about 3 $\mu J/cm^2$. Scatter from the 400 nm pump pulse was removed with a 450 nm long-wavelength filter coupled with Schott glass OG 420 and OG 570 filters. For the low-temperature experiments, the cryostat was cooled with liquid He, and the temperature was measured and controlled with a Lakeshore 321 controller.

Time resolved pump−probe diffuse reflectance experiments[17−19] were performed on a 1 kHz Coherent Libra laser system equipped with a Helios transient absorption spectrometer (Ultrafast Systems). A small portion of the 800 nm fundamental was focused onto a sapphire plate to generate a white light continuum pulse, which was used as the probe. The remaining 800 nm fundamental was frequency-doubled to 400 nm and used as the pump. Residual 800 nm light was removed from the pump pulse with Schott glass BG39 filters. The pump and probe were then focused onto the same spot on the surface of the powder sample. The scattered probe was collected with a 3 cm focal length lens and then coupled into the fiber optic cable of an Ocean Optics S2000 spectrometer. Scattered pump light was blocked with a 400 nm long-wavelength pass filter and a Schott glass OG 420 filter before the detector. The spectrometer and the motorized stage used to vary the pump path length were controlled with the Helios software. The typical per-pulse pump fluence for these experiments was 6 $\mu J/cm^2$. The highly scattering samples used for diffuse reflectance experiments typically reduce the temporal resolution below that which would be expected based on the laser pulse width.[17] We estimate that the temporal resolution of our system is ∼1.5 ps based on the rising edge of the TA signal.

RESULTS AND DISCUSSION

When pyrene and TCNQ are mixed together in an organic solvent, they can associate to form a weakly bound complex with new absorption features that extend into the near-infrared. Figure 2 shows the absorption spectra of the donor pyrene, the acceptor TCNQ, and the two new absorption bands at ∼500 and 760 nm that arise from the CT absorption features of the donor−acceptor complex formed at high concentrations in $CHCl_3$ solution. By varying the concentrations of the molecular components, both *K*, the equilibrium constant for CT complex formation, and its absorption coefficient $\varepsilon(\lambda_{CT})$ can be determined. As shown by previous workers, in the limit where the amount of CT formation is small relative to the monomer concentrations but its absorbance $Abs(\lambda_{CT})$ is measurable, one can derive the following expression[20]

$$\frac{Abs(\lambda_{CT})}{[Py]_0[TCNQ]_0} = K\left(\varepsilon(\lambda_{CT}) - \frac{Abs(\lambda_{CT})}{[TCNQ]_0}\right) \quad (1)$$

where $[Py]_0$ and $[TCNQ]_0$ are the initial concentrations of the donor pyrene and acceptor TCNQ, respectively. A Scatchard plot of $Abs(\lambda_{CT})/[Py]_0[TCNQ]_0$ versus $Abs(\lambda_{CT})/[TCNQ]_0$ should result in a straight line where the slope is $-K$ and the *y*-intercept is $K\varepsilon(\lambda_{CT})$. By measuring the absorbance at 760 nm

dx.doi.org/10.1021/jp302829a | J. Phys. Chem. A XXXX, XXX, XXX−XXX

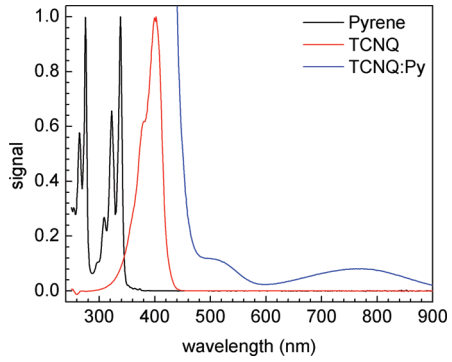

Figure 2. Steady-state absorption of monomeric pyrene (black), monomeric TCNQ (red), and a mixture of 0.37 mM TCNQ and 12 mM pyrene (blue) in $CHCl_3$. The plots for pyrene and TCNQ have been normalized to their peak emissions. In a mixed solution, the monomer absorptions dwarf that of the CT complex, owing to its low epsilon and association constant.

as a function of pyrene and TCNQ concentration, the data in Figure 3 are obtained, where K = 13.1 ± 0.2 and ε(760 nm) =

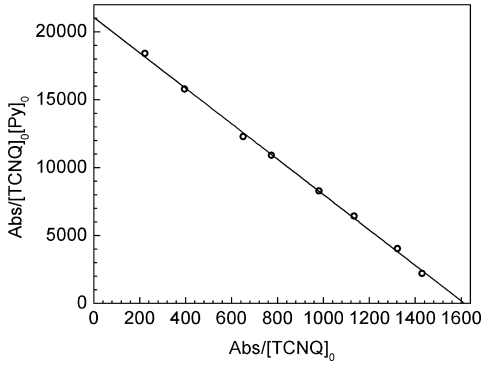

Figure 3. Scatchard plot for pyrene/TCNQ complex formation in $CHCl_3$. The relationship was linear over a saturation fraction range of 0.14–0.90, indicative of the exclusive formation of 1:1 complexes. From the slope and x-intercept of this graph, K and ε were determined to be 13.1 ± 0.2 and 1610 ± 30 L mol^{-1} cm^{-1} at 760 nm, respectively, as described in the text.

1610 ± 30 M^{-1} cm^{-1} are obtained. Our values differ slightly from those previously obtained by Ayad et al., who varied the TCNQ concentration over a more limited range.[21] To acquire data across a larger range of saturation fractions (the fraction of complexed species), we varied the pyrene concentration instead. We did not see any evidence of nonstoichiometric complexation in our absorption spectra, and the linearity of the Scatchard plot corroborated this.

The solution absorption spectrum bears a close resemblance to that obtained for the CT crystal. Figure 4 shows the absorption spectrum of a film of pyrene/TCNQ microcrystals of pyrene/TCNQ, which shows the same broad bands at 500 and 760 nm as seen in the 1:1 solution complex. The location of these bands also agrees well with the absorption line shape derived by Tanaka from a Kramers–Kronig analysis of the single-crystal reflectance spectrum.[15] Due to their strong absorption that extends across the visible and into the near-infrared, these crystals appear black. The major difference between the solution complex and the crystal is that the solid exhibits measurable fluorescence. The luminescence spectrum of a pyrene/TCNQ crystal is also shown in Figure 4, centered

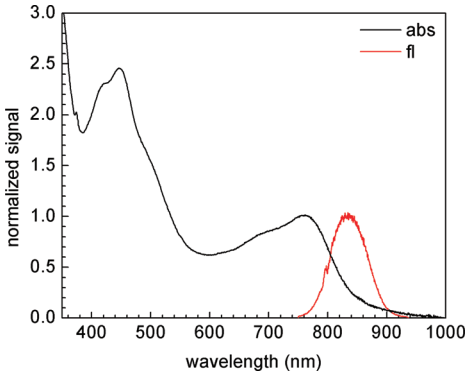

Figure 4. Absorption spectrum of a polycrystalline thin film and the fluorescence spectrum of a single crystal.

at 840 nm. The broad, red-shifted emission is characteristic of these CT compounds in the solid state. Note that no measurable fluorescence was observed for the pyrene/TCNQ complex in solution, where the absence of a rigid matrix appears to facilitate very rapid charge recombination and nonradiative relaxation, effectively quenching the fluorescence. Rapid charge recombination has been observed for CT complexes in liquid solutions,[9] and this helps explain the absence of fluorescence, even for compounds that are emissive in the solid state.[22]

In order to investigate the mechanism of charge recombination in the solid state, we wanted to use the fluorescence decay as a measure of the recombination rate. However, to do this, we first had to investigate whether our pyrene/TCNQ samples demonstrated the same sensitivity to laser and mechanical damage as the previously studied TCNB complexes.[13] Figure 5a compares the normalized fluorescence decay of a pyrene/TCNQ single crystal before and after a 60 s laser exposure totaling 99 mJ/cm^2 at 400 nm. This fluence would have had a severe effect on the observed fluorescence decay of pyrene/TCNB but has no effect on the decay rate of pyrene/TCNQ. The same resistance to photodamage was also observed in powders and microcrystals of pyrene/TCNQ. In all cases, the only effect of prolonged laser exposure was a decrease in overall signal level but no change in the kinetics. The second question concerns the comparison of powder and single-crystal spectroscopic data. Because transient absorption experiments may only be performed on powdered samples due to the high optical density of single crystals, a comparison of luminescence decays with transient absorption dynamics requires that the two types of samples demonstrate the same behavior. When $BaSO_4$ was used as the inert filler, a nonexponential tail was observed in the fluorescence decay, in contrast to the purely single-exponential decay seen in the neat crystals. When Teflon beads were used as the filler material, the tail was no longer present in the powder data. Figure 5b compares the decays obtained from the fluorescence of the single crystal and the powder sample in Teflon, both of which yield the same exponential relaxation time of 290 ps to within the experimental error. The results in Figure 5a and b establish that the kinetic results from the Teflon powdered crystal are applicable to the single crystal; mechanical grinding and photodamage do not induce new kinetic relaxation pathways, unlike in the TCNB CT crystals studied previously. A second advantage of the pyrene/TCNQ system is its single-exponential fluorescence decay and lack of spectral changes during the decay. The simple decay dynamics, indicative of a

dx.doi.org/10.1021/jp302829a | J. Phys. Chem. A XXXX, XXX, XXX–XXX

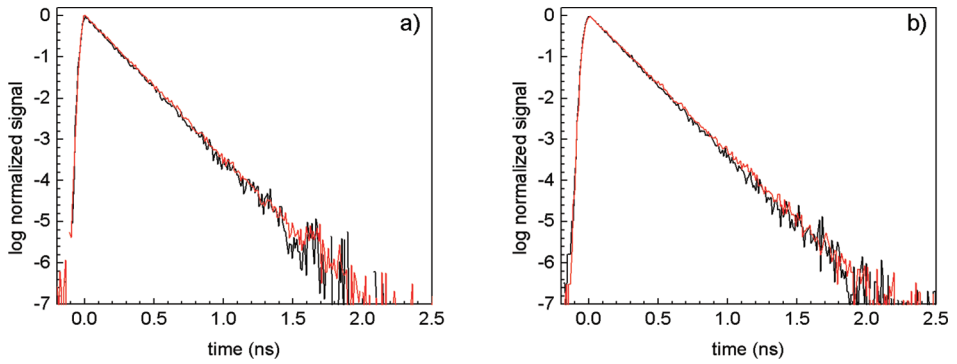

Figure 5. (a) Fluorescence decay kinetics of a pyrene/TCNQ single crystal before (black) and after (red) a 60 s laser exposure of 99 μJ/cm^2. The signal level decreased, but the decay kinetics were unchanged. (b) Comparison of the fluorescence decays for a single crystal (black) and a 2% by weight Teflon powder sample (red).

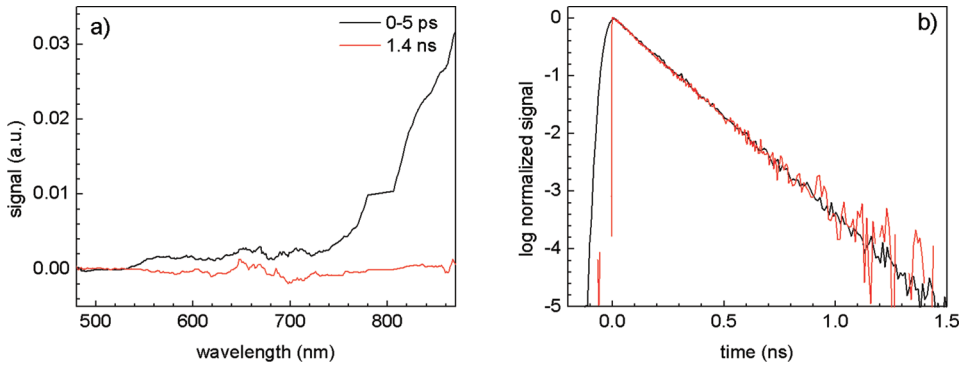

Figure 6. (a) Transient absorption spectra of the powder sample at early (0−5 ps, black) and late (1.4 ns, red) delays. (b) Comparison of the fluorescence decay of a single crystal (black) and the transient absorption decay at 820 nm of a powdered sample (red). Both signals decay with the same 290 ps time constant.

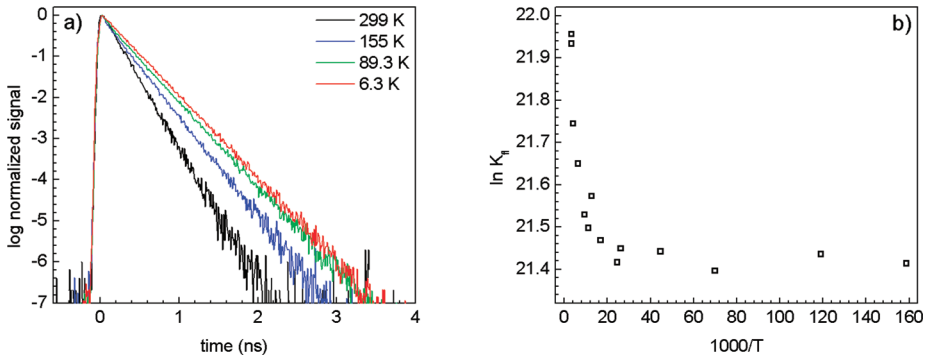

Figure 7. (a) Crystal fluorescence decay at different temperatures. Below 60 K, the decay ceases to change. (b) Arrhenius plot for the fluorescence decay rate k_{fl} versus inverse temperature, showing the crossover from activated to tunneling regimes.

single excited-state species, is in contrast to that of some TCNB crystals, where multiple emissive species can contribute to the decays.[13,23]

Transient absorption experiments were performed on the powdered CT sample in order to determine whether the fluorescence decay was due to relaxation back to the ground state or into other types of long-lived excited states like triplets or separated charges. Such states are nonfluorescent but should manifest themselves in the TA experiment as long-lived induced absorption features or as a bleach of the CT absorption. In Figure 6a, the early (0−5 ps) and late (1400 ps) transient absorption spectra measured for the powdered sample are shown. Immediately after photoexcitation, there is an induced absorption that extends across the visible range but peaks past 800 nm. The strong absorption at longer wavelengths is consistent with the shape of the TCNQ radical anion absorption that has been observed in other experiments.[24−26] Although the 400 nm pump pulse would be expected to excite at least some neutral states, for example, the TCNQ monomer, the formation of the CT state occurs within the time resolution of our measurement. We did not resolve any evolution of the TA spectrum within the 0−10 ps time window, other than the beginning of the slow decay. Rapid formation of the CT state after excitation of neutral states is consistent with results on other CT crystal systems.[9−11] Here, we are more concerned with the rate of the reverse reaction, recombination of the separated charges. We can follow this process by monitoring the absorption feature at ∼820 nm,

dx.doi.org/10.1021/jp302829a | J. Phys. Chem. A XXXX, XXX, XXX−XXX

which decays away completely by 1400 ps. After the absorption decays, there is no residual bleach or induced absorption that would indicate the presence of other species. When the decay of the anion TA signal at 820 nm is compared to that of the fluorescence, they overlap perfectly, as shown in Figure 6b. The two different time-resolved experiments, fluorescence and transient absorption, give consistent results, indicating that the initially created CT state decays back to the neutral ground state via a single-step process, without the measurable formation of long-lived intermediate or dark states like triplets or free carriers.

The data in Figure 6 establish that the fluorescence decay of pyrene/TCNQ reflects relaxation from the CT state back to the neutral ground state and that other relaxation channels play negligible roles. The last question that we need to address is the mechanism of this relaxation. First, we fit the lowest-energy CT absorption band in Figure 2 to a Gaussian line shape function and use the Strickler–Berg relation[27] to estimate the radiative decay time τ_{rad}. Integration of $\varepsilon(\nu)$ from 600 to 900 nm yields τ_{rad} = 220 ns. This value is almost 10^3 times larger than the observed τ_{fl}, indicating that the excited-state relaxation is dominated by nonradiative charge recombination. The fluorescence lifetime is only weakly dependent on temperature, as shown in Figure 7a, but remains single exponential at all temperatures. An Arrhenius plot of $\ln(k_{fl})$ versus $1000/T$ is shown in Figure 7b. At high temperatures, the linear slope of this curve indicates a thermally activated process, and in the range of 300–60 K, we extract an activation energy of 0.2 kJ/mol. However, after 60 K, the curve levels out and $k_{fl} = 3 \times 10^9$ s^{-1} becomes independent of temperature. As mentioned above, this temperature-independent rate is orders of magnitude larger than the radiative decay rate. Non-Arrhenius behavior in electron-transfer systems can result from several different phenomena, including coupling to high-frequency vibrational modes,[28−30] the influence of motions on widely separated time scales,[31,32] and nonergodic effects.[33] Distinguishing among these different but related mechanisms would require a detailed study, coupled with theoretical calculations, which is beyond the scope of this paper. However, this temperature-dependent behavior is very similar to what has been observed in other CT systems and attributed to tunneling.[34−39] Assuming that this is the case, then the transition between Arrhenius and non-Arrhenius behavior that occurs at $T_{cross} \approx 60$ K can provide some clue as to the mechanism. If we use Buhks and Jortner's theory for the transition between the quantum and classical rate regimes,[40,41] in the strong-coupling regime, this crossover should take place when

$$T_{cross} \approx \frac{\hbar\omega}{4k_B} \tag{2}$$

where ω is the frequency of the generalized nuclear coordinate for the reaction and k_B is Boltzmann's constant. From this relation, we find $\omega \approx 170$ cm^{-1}. The nuclear coordinate that is coupled to the charge recombination is unknown but probably involves the intermolecular separation of the donor and acceptor within the crystal lattice. Resonance Raman data for a closely related crystal system, perylene/TCNQ, indicates the presence of multiple intermolecular phonon modes in this frequency range.[42]

CONCLUSION

In this paper, we have extended our previous studies on the excited-state relaxation in molecular CT crystals. Unlike the donor/TCNB cocrystals that we investigated in a previous paper, the pyrene/TCNQ cocrystal shows simple kinetics that are robust with respect to both laser damage and mechanical perturbation. This material exhibits two CT transitions that extend its absorption into the near-infrared. Using a combination of picosecond photoluminescence and femtosecond transient absorption, we confirm that relaxation of the lowest-energy CT state proceeds by nonradiative electron–hole recombination back to the neutral ground state. The recombination rate exhibits a transition from Arrhenius to non-Arrhenius behavior at 60 K. We interpret this temperature dependence in terms of a thermally activated tunneling mechanism and estimate that it is mediated by a vibration in the range of 170 cm^{-1}, consistent with the known phonon modes of similar crystals. Despite its low band gap, pyrene/TCNQ is not a good analogue for polymer bulk heterojunction systems because it does not appear that the initially separated charges are able to diffuse away from each other. Instead, the charges recombine on a subnanosecond time scale in a process mediated by tunneling. It is possible that the pyrene/TCNQ cocrystal could provide a structurally well-defined condensed-phase system with which to test various theories of electron transfer. The positions of both the donor and acceptor are well-defined, their electronic properties are well-studied, and the charge recombination rate can be measured unambiguously by spectroscopic means.

AUTHOR INFORMATION

Corresponding Author

*E-mail: christopher.bardeen@ucr.edu.

Notes

The authors declare no competing financial interest.

ACKNOWLEDGMENTS

This research was supported by the Department of Energy, Basic Energy Sciences, Grant DOE-FG02-09ER16096. Time-resolved measurements were performed on an instrument purchased with support from the National Science Foundation, Grant CRIF-0840055.

REFERENCES

(1) Wright, J. D. *Molecular Crystals*, 2nd ed.; Cambridge University Press: Cambridge, U.K., 1995.
(2) Hosaka, N.; Obata, M.; Suzuki, M.; Saiki, T.; Takeda, K.; Kuwata-Gonokami, M. *Appl. Phys. Lett.* **2008**, *92*, 113305/113301–113305/113303.
(3) Al-Kaysi, R. O.; Muller, A. M.; Frisbee, R. J.; Bardeen, C. J. *Cryst. Growth Des.* **2009**, *9*, 1780–1785.
(4) McConnell, H. H.; Hoffman, B. M.; Metzger, R. M. *Proc. Natl. Acad. Sci. U.S.A.* **1965**, *53*, 46–50.
(5) Ojima, S.; Miyasaka, H.; Mataga, N. *J. Phys. Chem.* **1990**, *94*, 7534–7539.
(6) Hubig, S. M.; Bockman, T. M.; Kochi, J. K. *J. Am. Chem. Soc.* **1996**, *118*, 3842–3851.
(7) Nicolet, O.; Vauthey, E. *J. Phys. Chem. A* **2002**, *106*, 5553–5562.
(8) Mohammed, O. F.; Vauthey, E. *J. Phys. Chem. A* **2008**, *112*, 5804–5809.
(9) Fukazawa, N.; Fukamura, H.; Masuhara, H.; Prochorow, J. *Chem. Phys. Lett.* **1994**, *220*, 461–466.
(10) Asahi, T.; Matsuo, Y.; Masuhara, H. *Chem. Phys. Lett.* **1996**, *256*, 525–530.

(11) Asahi, T.; Matsuo, Y.; Masuhara, H.; Koshima, H. *J. Phys. Chem. A* **1997**, *101*, 612−616.
(12) Hubig, S. M.; Kochi, J. K. *J. Phys. Chem.* **1995**, *99*, 17578−17585.
(13) Dillon, R. J.; Bardeen, C. J. *J. Phys. Chem. A* **2011**, *115*, 1627−1633.
(14) Prout, C. K.; Tickle, I. J.; Wright, J. D. *J. Chem. Soc., Perkin Trans.* **1973**, *2*, 528−530.
(15) Tanaka, M. *Bull. Chem. Soc. Jpn.* **1978**, *51*, 1001−1008.
(16) Vincent, V. M.; Wright, J. D. *J. Chem. Soc., Faraday Trans. 1* **1974**, *70*, 58−71.
(17) Asahi, T.; Furube, A.; Fukumura, H.; Ichikawa, M.; Masuhara, H. *Rev. Sci. Instrum.* **1998**, *69*, 361−371.
(18) Colombo, D. P.; Bowman, R. M. *J. Phys. Chem.* **1996**, *100*, 18445−18449.
(19) Kamat, P. V.; Gevaert, M.; Vinodgopal, K. *J. Phys. Chem. B* **1997**, *101*, 4422−4427.
(20) Deranleau, D. A. *J. Am. Chem. Soc.* **1969**, *91*, 4044−4049.
(21) Ayad, M. M.; El-Daly, S. A. *Z. Phys. Chem.* **1995**, *190*, 211−221.
(22) Short, G. D.; Parker, C. A. *Spectrochim. Acta, Part A* **1967**, *23*, 2487−2489.
(23) Betz, E.; Port, H.; Schrof, W.; Wolf, H. C. *Chem. Phys.* **1988**, *128*, 73−81.
(24) Vandevyer, V.; Richard, J.; Barraud, A.; Ruaudel-Teixier, A.; Lequan, M.; Lequan, R. M. *J. Chem. Phys.* **1987**, *87*, 6754−6763.
(25) Shida, T. *Electronic Absorption Spectra of Radical Ions*; Elsevier: New York, 1988.
(26) Cho, K. S.; Nam, Y. S.; Kim, D.; Lee, W. H.; Choi, J. W. *Synth. Met.* **2002**, *129*, 157−163.
(27) Strickler, S. J.; Berg, R. A. *J. Chem. Phys.* **1962**, *37*, 814−822.
(28) Bixon, M.; Jortner, J. *J. Phys. Chem.* **1991**, *95*, 1941−1944.
(29) Liang, N.; Miller, J. R.; Closs, G. L. *J. Am. Chem. Soc.* **1990**, *112*, 5353−5354.
(30) Nan, G.; Wang, L.; Yang, X.; Shuai, Z.; Zhao, Y. *J. Chem. Phys.* **2009**, *130*, 024704/024701−024704/024708.
(31) Cukier, R. I. *J. Chem. Phys.* **1988**, *88*, 5594−5605.
(32) Dakhnovskii, Y.; Lubchenko, V.; Wolynes, P. *J. Chem. Phys.* **1996**, *104*, 1875−1885.
(33) Matyushov, D. V. *Acc. Chem. Res.* **2007**, *40*, 294−301.
(34) Barbara, P. F.; Meyer, T. J.; Ratner, M. A. *J. Phys. Chem.* **1996**, *100*, 13148−13168.
(35) Asahi, T.; Ohkohchi, M.; Matsusaka, R.; Mataga, N.; Zhang, R. P.; Osuka, A.; Maruyama, K. *J. Am. Chem. Soc.* **1993**, *115*, 5665−5674.
(36) Delaney, J. K.; Mauzerall, D. C.; Lindsey, J. S. *J. Am. Chem. Soc.* **1990**, *112*, 957−963.
(37) Kroon, J.; Oevering, H.; Verhoeven, J. W.; Warman, J. M.; Oliver, A. M.; Paddon-Row, M. N. *J. Phys. Chem.* **1993**, *97*, 5065−5069.
(38) Kuciauskas, D.; Liddell, P. A.; Lin, S.; Stone, S. G.; Moore, A. L.; Moore, T. A.; Gust, D. *J. Phys. Chem. B* **2000**, *104*, 4307−4321.
(39) Lemmetyinen, H.; Tkachenko, N. V.; Efimov, A.; Niemi, M. *J. Phys. Chem. C* **2009**, *113*, 11475−11483.
(40) Buhks, E.; Jortner, J. *J. Phys. Chem.* **1980**, *84*, 3370−3371.
(41) Milosavljevic, B. H.; Thomas, J. K. *J. Am. Chem. Soc.* **1986**, *108*, 2513−2517.
(42) Bandrauk, A. D.; Truong, K. D.; Carlone, C. *Can. J. Chem.* **1982**, *60*, 588−595.